

Removal of Direct Yellow 50 From Aqueous Solutions Using Chitosan-ISO-Vanillin Derivatives Chelating Polymers

Eman Alabbad (✉ ealabbad@iau.edu.sa)

Imam Abdulrahman Bin Faisal University

Research Article

Keywords: Adsorption, Chelating polymer, Chitosan-iso-vanillin resins, Direct Yellow 50 dye, Recycling, Wastewater treatment.

Posted Date: December 21st, 2020

DOI: <https://doi.org/10.21203/rs.3.rs-129329/v1>

License:  This work is licensed under a Creative Commons Attribution 4.0 International License.

[Read Full License](#)

**Removal of Direct Yellow 50 from aqueous solutions using chitosan-iso-vanillin derivatives chelating
polymers**

EMAN A. ALABBAD*

***Department of Chemistry, College of Science, Imam Abdulrahman Bin Faisal University, P.O. Box 1980,
Dammam 31441, Saudi Arabia.**

Correspondence author e-mail: ecalabbad@iau.edu.sa

Abstract

Background

Water contamination has increasingly become a significant problem affecting the welfare of living organisms perceived to be aquatic beneficiaries. The nature and origin of the contaminant always determines the purification techniques. The most common contaminants in wastewater include organic compounds such as dyes that must be eliminated to enhance water purity and safety.

Result

The results indicate that the removal of DY50 by the modified chitosan was affected by the solution pH, sorbent dosage, initial DY50 concentration, contact time, and temperature. The experimental data were fitted to the Langmuir, Freundlich, and Temkin isotherms, and Langmuir isotherm showed the best fit. The kinetic data were fitted to the pseudo-first-order and pseudo-second-order rate equations. The removal rate was 97.9% by chemisorption components after the three hours at about 0.05 g of sorbent dose and 100 ppm of the Direct Yellow 50 dye initial concentration. The adsorption behavior of the modified chitosan for the removal of DY50 was well-described using the pseudo-second-order kinetic model, Intraparticle diffusion analysis was also conducted. The thermodynamic properties such as free energy (ΔG), enthalpy (ΔH), and entropy (ΔS), in addition to the intraparticle diffusion rate were similarly defined.

Conclusion

The pH, initial DY50 concentration, sorbent dosage, adsorption temperature, and contact time had a significant effect on the adsorption of DY50 by chitosan-iso-vanillin.

	28
Keywords: Adsorption, Chelating polymer, Chitosan-iso-vanillin resins, Direct Yellow 50 dye, Recycling,	29
Wastewater treatment.	30
1. INTRODUCTION	31
Water pollution is a significant problem encountered worldwide. The leading water pollution causes are	32
human activities such as mining, marine dumping, oil leakages, burning fossil fuels, industrial wastes, and waste	33
from the sewer line [1]. Water contaminant includes organic compounds such as dyes that must be eliminated to	34
enhance water purity and safety [2]. Numerous water purification methods like ozonation, reverse osmosis,	35
adsorption, coagulation, and flocculation exist [3]. However, removing harmful and poisonous substances is	36
always defined by the nature and origin of the contaminant and treatment cost [4] As a result, simple, cost-effective,	37
and efficient biological and physical water treatment techniques have been developed to enable water recycling.	38
The toxicity, bioaccumulative nature, and environmental persistence of heavy metals make them typical	39
environment pollutants [5]. Since the contamination of water and soil with heavy metals results in serious health	40
concerns, their removal is essential to all living things' health. In recent years, Chitosan has become a frequent	41
focus of many studies as an adsorption material. Its comparatively low-cost, non-toxicity, ease of degradation,	42
good biocompatibility, rich resources, and hydrophilicity make it a useful water treatment agent [6]. Chitosan has	43
great hydroxyl numbers and amino compounds that enhance its ability to absorb metal ions like Cr, Pb, Cu, Ni,	44
and Zu [7]. Also, it has a malleable polymer structure that increases metal ions' complexation.	45
Iso-vanillin is a phenol derivative, an organic compound, and vanillin isomer. Organic compounds are	46
chemical compounds containing carbon-hydrogen bonds, and isomers are molecules whose molecular formula is	47
identical. In previous study notes that vanillin derivatives have been used to prepare organometallic polymers [2].	48
A recent investigation of chitosan-ortho-vanillin polymers in removing cadmium ions from solutions whose	49
solvent is water found that it had an impulsive adsorption process and the removal capacity was maximum.	50
This study examined the application of cost-effective chitosan-iso-vanillin compound in the elimination	51
of Direct Yellow 50 dye from wastewater. The research conducted numerous symmetric exercises to regulate the	52
kinetic and thermodynamic factors. A chitosan-iso-vanillin polymer was used to eliminate the Direct Yellow 50	53
dye impurities from the wastewater. The pollutant elimination efficiency, adsorption capacity, and sorption	54
mechanism of the aqueous DY50 dye by the chitosan-iso-vanillin were determined.	55
2. METHODS AND EXPERIMENTAL	56

Nearly every compound applied in the experiment, such as the DY50 dye (Merck), methanol (99%), ethanol (99%), iso-vanillin (99%), glacial acetic acid (99%), and acetone (99%), chitosan (not less than 85% glucosamine), were acquired from the commercial outlets and applied similarly. Additionally, a pH meter (Metrohm, 525A), a UV-scanning spectrophotometer UVD-2950 (LABOMED, INC), and an orbital shaker stabled at 757 were used in the examination of the exercise.

2.1. Synthesis of chitosan-iso-vanillin biosorbent

Chitosan-iso-vanillin was formed and characterized according to a process in the literature [8]. An adsorbent substance was obtained by refluxing 5.70 g of chitosan with a solution containing about 13.69 g of the iso-vanillin monomer, 90 mL methanol, and 9 mL glacial acetic acid. The experimental design enabled the removal of dyes [9,10]. The compounds acetone and ethanol were used to wash and filter the obtained material through the Soxhlet extraction method. The final stage involved desiccated sorbent performed at a temperature of about 70 °C during the night.

2.2. Preparation of DY50 dye solution

No additional purification, such as acid dye, was applied to prepare the DY50 standard solution. The solution was made by dissolving powdered DY50 in distilled water, forming a compound of chemical formula $C_{35}H_{24}N_6Na_4O_{13}S_4$. Similarly, sequential dilution was conducted to obtain the other several with a concentration of 1,3,5,7,10,15,20, and 30 ppm. The numerous concentrations obtained were used to provide standardization of the adsorption curve about the anticipated wavelength (λ) concentration of about 412 nm. From the calibration curve, the precise concentrations of the unidentified dye solutions were identified and measured. The polymer structure defined the complexity of the metal ion. The DY50 dye compound structure is shown in **Fig 1**.

2.3. Sorption of DY50 dye solution onto polymer materials

The batch equilibrium reaction was applied to examine the elimination of dye. Procedurally, about 25 mL of DY50 was the solution titrated into the 100 mL flask and suspended for about 3 h at temperature 30 °C in the presence of 0.05g sorbent. The 0.1 M NaOH and 0.1 M HCl were used to regulate the pH scale at various time intervals, for instance, 5, 10, 20, 60, 120, 240, 480, and 1440 min. The impact of contact time was assessed during the elimination of dye [11,12]. Similarly, additional practical was performed at varying DY50 dye concentration and temperature, for example, 20, 30, 40, 50, 70, 100, and 150 mg. L⁻¹ and 20 °C, 30 °C, 50 °C, and 70 °C parameters, respectively. The polymer enhanced elimination of metal ion [13]. Similarly, various weights of 0.01,

0.05, 0.1, 0.2, and 1.0 g of the dehydrated adsorbent were used to examine the impact of the polymer present. After that, solutions were filtered to obtain the DY50 concentration remains [1,14,15]. The UV-Vis spectroscopy was applied to determine the quantity. The quantity of DY50 ions in equilibrium denoted by (Q_e) was calculated, as shown in the Eq. (1):

$$Q_e = \frac{(C_o - C_e)V}{W} \quad \text{where } Q_e = \text{mg DY50 adsorbed/g sorbent} \quad (1)$$

Similarly, C_o and C_e denote both initial and equilibrium dye concentration (mg. L^{-1}), W is polymer quantity (g), and V represents the volume of the dye (L).

At every time interval, the quantity of DY50 remains were eliminated by the Eq. (2):

$$Q_t = \frac{(C_o - C_t)V}{W} \quad (2)$$

Whereby C_t denotes the DY50 solution concentrations (mg. L^{-1}) at various period intervals (t).

3. RESULTS AND DISCUSSION

3.1. Synthesis and characterization of biosorbent

Chitosan is among the most readily available biopolymer. The compound has various behavioral characteristics such as the capability to form mechanical membranes, non-toxicity nature, antimicrobial activity, and biocompatibility, thus influencing its massive food engineering application. The technique has helped in water purification, food preservation, and fruit juice isolation, among other activities [16-18]. Similarly, the polymer can be used in an organized delivery system through the microsphere/ionosphere method. The polymer involves cross-linking to advance the reacting agents' specific and time frame activities like glutaraldehyde, formaldehyde, and glyoxal. Additionally, both the bean and orchid vanilla were also applied to purify and flavoring nutrients due to their safety. The substance also displays additional bioactive properties [2,19,20]. The combination of both the chitosan and vanillin facilitated a strong structure that regulated adsorbates release due to the Schiff-base reaction between the two products. It was due availability of amino and aldehyde substances in the compound's chitosan and vanillin, respectively. After the Schiff base formation, the other reaction was induced between chitosan and iso-vanillin to form the adsorbent component, as shown in **Fig 2**.

3.2. Effect of pH on DY50

The solution's pH influence on the DY50 sorption was between 3.0 to 10.0pH. DY50 solution's pH value plays a significant role in adsorption as it influences functional groups' dissociation both on the active sites and

adsorbent's surface charge and the DY50 solution's chemistry [21]. As the pH value increased, the amount of DY50 adsorbed by chitosan-iso-vanillin decreased. The optimum level of adsorption (97.3%), mass 0.05g, was recorded at a pH value of 3.0. Previous study reports that other studies found that when chitosan-iso-vanillin is used as an adsorbent, optimum pH ranged between 3 to 6 [2]. As **Fig 3.** illustrates, the adsorbent used was able to remove DY50 at a stable rate across various pH levels. Based on the results, two deductions can be made. First, an aqueous solution dissolves DY50 dye resulting in the separation of sulfonate groups ($R - SO_3Na$) from the dye and the addition of anionic dye ions. Second, the electrostatic attraction between the methyl orange ions and the adsorbent's surface successfully removes the dye. Increasing the dye resulted in a decrease in the adsorption [22]. The change was due to the competition between OH ions in the aqueous solution with the DY50 anions.

3.3. Influence of DY50 concentration and isothermal study

Fig 4. shows that an increase in the initial DY50 concentration leads to an increased dye adsorption capacity onto chitosan-iso-vanillin. The initial amount of molecules in the dye over the available adsorption sites decreased at low concentrations. As a result, more adsorption sites became known to the dye molecules. The adsorption rate was affected by the initial DY50 concentration that also influenced the sorbent adsorption capacity [21,23]. The impact was induced by a rise in a concentration gradient that resulted in a similar surge in initial DY50 concentration. However, the number of adsorption sites reduced at high initial dye concentration due to a rise in dye molecules concentration [24,25]. It can be summarized that the ratio of adsorption areas to the dye molecules' initial quantity was equal at low concentration [26]. The anionic dye adsorption level was increased by protonation. The figure below graphically demonstrates the impact of the initial concentration.

This can be summarized by the fact that at low concentrations, the ratio of the initial number of dye molecules to the available adsorption sites is low; therefore, more adsorption sites are available for the dye molecules, and the removal rate increases. However, at higher concentrations, the ratio of the initial number of available adsorption sites to the dye molecules is low; therefore, the number of available adsorption sites becomes lower, and the dye removal decreases. Proton effectively improved the adsorption of the anion dye onto chitosan [27].

The adsorption of DY50 onto chitosan-iso-vanillin was explained using a linear plot of the Langmuir, Freundlich, and Temkin isotherm models. The current study demonstrated the distribution method of the adsorbed molecules in the equilibrium state between both the solid and liquid phases, which is referred to as isotherm adsorption.

The Langmuir isotherm model is shown by Eq. (3):

$$C_e/Q_e = 1/(Q_0 K_L) + C_e/Q_0 \quad (3)$$

K_L and Q_0 were the coefficients of the Langmuir adsorption model, and they are related to sorption energy (L/mg) and adsorption capacity (mg/g), respectively.

Furthermore, R_L , a dimensional constant separation factor, was used to express those basic properties of the Langmuir isotherm model and was defined as Eq. (4):

$$R_L = \frac{1}{1 + K_L C_e} \quad (4)$$

The isotherm can be estimated based on the value of R_L , where if $R_L = 1$, the isotherm is linear, if greater than one is unfavorable, either ($0 < R_L < 1$) is favorable or ($R_L = 0$) is irreversible.

The Freundlich model, which is acceptable at low concentrations and heterogeneous surfaces, is expressed by Eq. (5):

$$q_e = K_F C_e^{\frac{1}{n}} \quad (5)$$

The coefficients of the Freundlich adsorption model are n and K_F represented the adsorption capacity and degree of adsorption correspondingly. It could also be defined by the intercept and gradient of the linear plot $\log q_e$ versus $\log C_e$.

The Temkin model includes the effects of indirect adsorption/desorption reactions on the adsorption temperature.

The hypothesis of this model is based on the fact that the adsorption process decreases the adsorption heat of all molecules linearly. The Temkin isotherm can be calculated by Eq. (6):

$$q_e = \frac{RT}{b} \ln AC_e \quad (6)$$

where the constant $b = RT/\Delta E$, T is the temperature in K, the general gas constant is $R = 8.314$ J/mol K, Temkin equilibrium constant (L/mg) = A (maximum binding energy), variation adsorption energy (J/mol) $\Delta E = (-\Delta H)$, A is the Temkin equilibrium, and the adsorption (maximum) capacity is Q_0 [28,29].

A and b from the intercept and the slope of plot q_e against plot $\ln C_e$ are shown in Table 1. The isotherm parameters R^2 of the Langmuir, Freundlich, and Temkin models were 0.9886, 0.9779, and 0.9771, respectively. Also, the adsorption coefficient (K_L) was 0.2259 and the maximum removal capacity Q_0 was 250 mg.g⁻¹. The constant K_F

of the Freundlich isotherm, which reflects the capacity of the adsorption, was 43.7219 mg/g. Also, the adsorption was measured using the Temkin isotherm model, which suggests that the energy of the adsorption decreases because of the increase in the surface coverage by the DY50 ions by the regular distribution of the binding energies to a maximum; the sorption process can be visualized based on this model. In this study, the Langmuir isotherm was a favorable model that most suitable the equilibrium data across the adsorption isotherm [30].

3.4. Effect of Adsorbent Dosage.

The dosage test was also conducted in the study to determine the adsorption rate of the DY50. The variation of sorbet quantity was done from 0.01 g to 0.2 g. It was noted that the elimination of dye only occurred at 0.01 and 0.05 g, with rates 93.12% and 97.80%, respectively. The dye's removal rate varied with bio-sorbent dosage until the attainment of quantity 0.2g with the elimination rate of 97.92%. The number of adsorption areas was also noted to have risen probably due to the molecules' clumping or intersection. Similarly, it is employed to treat acute cadmium infections [26]. The impact of adsorbent dosage on DY50 results was obtained and graphically demonstrated, as shown in **Table 2** and **Fig. 5**, respectively. Table 2 shows a change in the absorbent dose from 0.01g to 0.3g and its effect on the removal of DY50. As observed from Table 2, the lowest removal rate of DY50, 93.12%, was in 0.01 g of bio-sorbent, whereas 0.05g and 0.2 g of bio-sorbent showed a removal rate of 97.80% and 97.92%.

Table 2 and **Fig. 5** reveal increasing the removal rate of DY50 with an increase in the bio sorbent dose until it attained a plateau at 0.3 g, where the removal rate was 98.04%. The rise may be due to the increase in the adsorption surface and increased frequency of the adsorption sites' availability. Despite improving the DY50 removal rate, a further increase in the adsorbent dosage did not affect the adsorption rate proportionally but caused an increase in the adsorption sites' availability. The overlapping of adsorption sites possibly causes this, hence an increase in the diffusion path length.

3.5. Influence of sorption period and kinetic analysis

Another variable that affects the adsorption process is the sorption period; the kinetic analysis during this period is shown in **Fig 6**. This figure shows that the adsorption time caused a rapid uptake of DY50 by chitosan-iso-vanillin. Initially, the rate was high owing to the high electrostatic attraction on the surface of the adsorbent. An increase in the concentration of DY50 increased the time required to reach equilibrium; thus, the contact time is an important variable in the adsorption process [12,31]

The kinetic data were processed via two adsorption patterns: the pseudo-first and second kinetic orders shown in Eq. (7) and Eq. (8), respectively. The models of the pseudo-first and second kinetic orders could better describe the adsorption of dye on different sorbents [2].

$$\ln(Q_e - Q_t) = \ln Q_e - k_1 t \quad (7)$$

$$\frac{t}{Q_t} = \frac{1}{k_2 Q_e^2} + \frac{t}{Q_e} \quad (8)$$

The observed (Q_e) experimentally observed at 39.19 mg/L, the equilibrium was reached at 180 min, reflecting the occupation of the remaining active sites on the adsorbent surface. Specifically, the (R_2^2) of the pseudo-second order (0.9998) was greater than the (R_1^2) of the pseudo-first order (0.9798) in **Table 3**. The adsorption of DY50 by chitosan-iso-vanillin approached balance rapidly, and the adsorption surface was densely covered. Subsequently, the surface was gradually blocked by the dye molecules, which increased the time needed to reach balance. These results are consistent with [15], in which the authors reported that the greater the concentration, the greater the time needed to reach equilibrium; that is, there is a direct relationship between these two parameters.

The rate constant was calculated via Eq. (9) to examine the adsorption mechanism as follows:

$$q_t = k_{id} t_{1/2} + c \quad (9)$$

where q_t the mass of DY50 in contact time t (min), k_{id} ($\text{mg} \cdot \text{g}^{-1} \cdot \text{min}^{-1/2}$) is the intra-particle diffusion rate constant and c is the boundary layer effect of adsorption. **Fig 7**. shows the linear plot q_t versus $t_{1/2}$ for DY50. The mechanism of intra-particle diffusion, which was not dominant in the rate-determining step, was illustrated using the correlation coefficient ($R^2 = 0.9785$) of the Weber-Morris model. Additionally, the adsorption occurs by diffusion in both the surface and intra-particles. In this study, the kinetic model of the pseudo-second order was dominant and, therefore, there was a direct adsorption rate control in the total kinetics of the sorption; this corroborated [32]. This result indicated that the electron exchange was controlled between adsorbates and adsorbents via chemical adsorption [33].

3.6. Influence of Temperature and Thermodynamic Investigation

The effect of temperature on the adsorption of DY50 by chitosan-iso-vanillin at pH=3 and the thermodynamic study are illustrated in **Fig. 8** The removal of DY50 was studied at four different temperatures (20, 30, 50, and 70

°C). The adsorption process was influenced by temperature; i.e., a change in temperature can change the equilibrium capacity of the adsorbent to adsorb a specific compound. An increase in temperature decreases the adsorption of the dye, representing the exothermic nature of the adsorption reaction, whereas a decrease in temperature represents its endothermic nature. The physical bonding between both organic compounds, including dyes and the active sites of adsorption, was weakened with increasing temperature, in addition to the low temperature of the adsorbed species and few available active sites [34,35]. However, the effect of temperature was negligible. This behavior was consistent with [36], in which the authors found that the removal of pigments may not be affected by a change in the temperature of wastewater. Therefore, temperature has a distinct effect on adsorption altering the adsorption equilibrium amplitude to adsorb certain compounds.

Thermodynamic factors like entropy (ΔS), enthalpy (ΔH), and free energy (ΔG) were employed to define the adsorption process changes the results are shown in **Table 4**. The increased value of free energy (ΔG) showed a positive impact of temperature on adsorption. According to previous research, enthalpy's (ΔH) negative value shows that the adsorption is exothermic. These parameters have been used to deduce the mechanism of adsorption **Table 4** shows that all ΔG values were negative, which indicated that the sorption was spontaneous and rapid at the four applied temperatures. Also, an increasing in temperature followed by an increase in the absolute value of ΔG may facilitate the adsorption process.

The exothermic or endothermic nature of the adsorption is based on the value of ΔH , which here is negative; this suggests that the adsorption was exothermic. Conversely, a positive ΔH value suggests another type of reaction, which is lined to heat. Consequently, positive values of entropy quantity (ΔS) may have been an indication of an enhanced disorder rate at the solid and liquid interface [37].

4. CONCLUSION

This study focused on examining the application of cost-effective chitosan-iso-vanillin compound in eliminating Direct Yellow 50 dye from wastewater and conducting numerous symmetric exercises to regulate the kinetic and thermodynamic elements. It was found that the adsorption temperature, pH, contact time, sorbent quantity, and DY50 dye concentration influenced the dye adsorption by chitosan-is-vanillin. Arguably, the sorbent applied attained a greater adsorption rate for the dye and model. The Langmuir was found to be the best isothermal model for data fixing. Additionally, this study discussed thermodynamics and changes in entropy (ΔS), free energy (ΔG), and enthalpy (ΔH). The adsorption involved both spontaneous and exothermic processes.

DECLARATIONS	236
Ethics approval and consent to participate	237
Not applicable.	238
Consent for publication	239
Not applicable.	240
Availability of data and materials	241
The data used to support the findings of this study are available from the corresponding author upon request	242
Competing of interests	243
Not applicable.	244
Funding	245
Not applicable.	246
Author's contributions	247
I am writing the main manuscript text and prepared figures and also reviewed the manuscript.	248
Acknowledgments	249
I give thanks to everyone who offered me support and encouragement throughout the study such as my lecturers, colleagues, and supervisors.	250 251
Author's information	252
Department of chemistry, College science, Imam Abdulrahman bin Faisal University, Dammam,31441, Saudi Arabia.	253 254
REFERENCES	255
[1] Crini G, Lichtfouse E. Advantages and disadvantages of techniques used for wastewater treatment. Environ Chem Lett. 2019; 17:145-55.	256 257
[2] Alabbad EA. Efficient removal of methyl orange from wastewater by polymeric chitosan-iso-vanillin. Open Chem J. 2020; 7: 16-25.	258 259

- [3] Sejie FP, Nadiye-Tabbiruka MS. Removal of methyl orange (MO) from water by adsorption onto modified local clay (kaolinite). *Phy Chem.* 2016; 6: 39-48. 260
261
- [4] Teodosiu C, Gilca AF, Barjoveanu G, Fiore S. Emerging pollutants removal through advanced drinking water treatment: a review on processes and environmental performances assessment. *J Cleaner Prod.* 2018;197: 262
1210-1221. 263
264
- [5] Ali H, Khan E, Ilahi I. Environmental chemistry and ecotoxicology of hazardous heavy metals: environmental persistence, toxicity, and bioaccumulation. *J Chem.* 2019; 2019:1-14. 265
266
- [6] Zheng X, Zheng H, Xiong Z, Zhao R, Liu Y, Zhao C, et al. Novel anionic polyacrylamide-modify-chitosan magnetic composite nanoparticles with excellent adsorption capacity for cationic dyes and pH-independent adsorption capability for metal ions. *Chem Eng J.* 2020; 392:123706. 267
268
269
- [7] Ma H, Kong A, Ji Y, He B, Song Y, Li J. Ultrahigh adsorption capacities for anionic and cationic dyes from wastewater using only Chitosan. *Journal of Cleaner Production.* 2019;214 :89-94. 270
271
- [8] Alakhras F, Al-Shahrani H, Al-Abbad E, Al-Rimawi F, Ouerfelli N. Removal of Pb(II) metal ions from aqueous solutions using chitosan–vanillin derivatives chelating polymers. *Pol. J. Environ. Stud.* 2019; 28: 272
1523-1534. 273
274
- [9] Arroub H, El Harfi A. Modeling and optimization of experimental parameters in the treatment of effluents by coagulation-flocculation processes: methodology of experimental design. *Mediterr J Chem.* 2018;7 :183- 275
197. 276
277
- [10] Joudi M, Mouldar J, Nasrellah H, El Mhammedi MA. Factorial experimental design for the removal of disperse dyes using hydroxyapatite prepared from Moroccan phosphogypsum. *Mediterranean Journal of Chemistry.* 2019; 8: 1-9. 278
279
280
- [11] Kang D, Yu X, Ge M, Lin M, Yang X, Jing Y. Insights into adsorption mechanism for fluoride on cactus-like amorphous alumina oxide microspheres. *Chem Eng J.* 2018; 345: 252-259. 281
282
- [12] Aichour A, Zaghouane-Boudiaf, H. Synthesis and characterization of hybrid activated bentonite/alginate composite to improve its effective elimination of dyes stuff from wastewater. *App Water Sci.* 2020; 10: 1-13. 283
284
- [13] Marasović K, Margeta J. A study of Roman water intake structures at the Jadro River's spring. *Vjesnik za arheologiju i historiju dalmatinsku,* 2017; 110: 509-532. 285
286
- [14] Kadiri L, Ouass A, Essaadaoui Y, Lebkiri A. *Coriandrum Sativum* seeds as a green low-cost biosorbent for methylene blue dye removal from aqueous solution: spectroscopic, kinetic and thermodynamic studies. *Mediterr J Chem.* 2018; 7: 204-216. 287
288
289

- [15] Ben W, Zhu B, Yuan X, Zhang Y, Yang M, Qiang, Z. Occurrence, removal and risk of organic micropollutants in wastewater treatment plants across China: Comparison of wastewater treatment processes. *Water Res*, 2018; 130: 38-46. 290
291
292
- [16] Meng B, Guo Q, Men X, Ren S, Jin W, Shen B. Modified bentonite by polyhedral oligomeric silsesquioxane and quaternary ammonium salt and adsorption characteristics for dye. *J Saudi Chem Soc*. 2020; 24: 334-44. 293
294
- [17] Tamer TM, Valachová K, Mohyeldin MS, Soltes L. Free radical scavenger activity of chitosan and its laminated derivative. *J Appl Pharm Sci*. 2016; 6: 195-201. 295
296
- [18] Eldin MS. Free radical scavenger activity of cinnamyl chitosan Schiff base. *J Appl Pharm Sci*. 2016; 6:130-6. 297
298
- [19] Nasrellah H, Yassine I, Hatimi B, Joudi M, Chema A, El Gaini L, et al. New synthesis of hydroxyapatite from local phosphogypsum. *J. Mater. Environ. Sci*. 2017; 83: 168-3174. 299
300
- [20] Padmavathy KS, Madhu G, Haseena PV. A study on effects of pH, adsorbent dosage, time, initial concentration, and adsorption isotherm study for the removal of hexavalent chromium (Cr (VI)) from wastewater by magnetite nanoparticles. *Procedia Technol*. 2016; 24: 585-94. 301
302
303
- [21] Huang R, Liu Q, Huo J, Yang B. Adsorption of methyl orange onto protonated cross-linked chitosan. *Arab J Chem*. 2017;10 :24-32. 304
305
- [22] Salgot M, Oron G, Cirelli GL, Dalezios N.R, Díaz A, Angelakis A.N. Criteria for wastewater treatment and reuse under water scarcity. Boca Raton FL, USA: CRC Press, 2016. 306
307
- [23] Al Hamouz, OCS. Synthesis and characterization of a novel series of cross-linked (phenol, formaldehyde, alkyldiamine) terpolymers for the removal of toxic metal ions from wastewater. *Arab J Sci and Eng*, 2016; 41: 119-33. 308
309
310
- [24] Laçin D, Aroguz AZ. Removal of dye pollution by modified halloysite as eco-friendly adsorbent. *The Int J Mater Eng Technol*. 2020; 3: 47-56. 311
312
- [25] Santhosh C, Daneshvar E, Kollu P, Peräniemi S, Grace AN, Bhatnagar A. Magnetic SiO₂@ CoFe₂O₄ nanoparticles decorated on graphene oxide as efficient adsorbents for the removal of anionic pollutants from water. *Chem Eng J*. 2017; 322: 472-487. 313
314
315
- [26] Zhou YS, Zeng RX, Zhang MZ, Guo LH. Treatment of an acute severe cadmium poisoning patient combined with multiple organ dysfunction syndromes by integrated chinese and western medicines: A case report. *Chin J Integr Med*. 2020; 26: 853-856. 316
317
318

[27] Zhai L, Bai Z, Zhu Y, Wang B, Luo W. Fabrication of chitosan microspheres for efficient adsorption of methyl orange. <i>Chin J Chem Eng.</i> 2018; 26: 657-666.	319 320
[28] Kundu S, Gupta AK. Arsenic adsorption onto iron oxide-coated cement (IOCC): regression analysis of equilibrium data with several isotherm models and their optimization. <i>Chem. Eng.</i> 2006; 122: 93-106.	321 322
[29] Hamdaoui O, Naffrechoux E. Modeling of adsorption isotherms of phenol and chlorophenols onto granular activated carbon: Part I. Two-parameter models and equations allowing determination of thermodynamic parameters. <i>J. Hazard. Mater.</i> , 2007; 147: 381-394.	323 324 325
[30] Saha TK, Bhounil NC, Karmaker S, Ahmed MG, Ichikawa H, Fukumori Y. Adsorption of methyl orange onto chitosan from aqueous solution. <i>J. Water Resour. Prot.</i> 2010; 2: 898-906.	326 327
[31] Alabbad EA. Estimation the sorption capacity of chemically modified chitosan toward cadmium ion in wastewater effluents. <i>Orient J Chem.</i> 2019; 35: 757-65.	328 329
[32] Plazinski W, Rudzinski W, Plazinska A. Theoretical models of sorption kinetics including a surface reaction mechanism: a review. <i>Adv. Colloid Interface Sci.</i> 2009; 152: 2-13.	330 331
[33] Habiba U, Siddique TA, Joo T, Salleh A, Ang B, Afifi A. Synthesis of chitosan/ polyvinyl alcohol/zeolite composite for removal of methyl orange, congo red and chromium (VI) by flocculation / adsorption. <i>J Carbohydr Polym.</i> 2017; 157: 1568-1576.	332 333 334
[34] Theydan SK. Effect of process variables, adsorption kinetics and equilibrium studies of hexavalent chromium removal from aqueous solution by date seeds and its activated carbon by ZnCl ₂ . <i>Iraqi Acad Sci. J.</i> 2018; 19: 1-12.	335 336 337
[35] Alqaragully MB. Removal of textile dyes (maxilon blue, and methyl orange) by date stones activated carbon. <i>Int. J Adv Res Chem Sci.</i> 2014; 1: 48-59.	338 339
[36] Li Q, Yue QY, Su Y, Gao BY, Sun HJ. Equilibrium, thermodynamics and process design to minimize adsorbent amount for the adsorption of acid dyes onto cationic polymer-loaded bentonite. <i>Chem Eng.</i> 2010; 158: 489-97.	340 341 342
[37] Kora AJ, Rastogi L. Catalytic degradation of anthropogenic dye pollutants using palladium nanoparticles synthesized by gum olibanum, a glucuronarabinogalactan biopolymer. <i>Ind Crops Prod.</i> 2016; 81: 1-10.	343 344
FIGURE LEGENDS	345
Fig 1: Structure of Direct Yellow 50 dye.	346
Fig 2: Structure of chitosan-iso-vanillin biosorbent.	347

Fig 3: Effect of pH on DY removal by chitosan-iso-vanillin (DY=40 ppm, T=30°C, W=0.05 g and t=3 h).	348
Fig 4: Effect of initial DY50 concentration on the equilibrium adsorption capacity of chitosan-iso-vanillin (W=0.05 g, pH=3, T=30°C, t=3 h).	349 350
Fig 5: Effect of biosorbent dose on DY removal (DY=40 ppm, pH=3, T=30°C, t=3 h).	351
Fig 6: Effect of contact time on DY50 removal by chitosan-iso-vanillin (DY=40 ppm, pH=3, T=30°C, W=0.05 g).	352 353
Fig 7: Fitting of DY adsorption data to the Weber-Morris intraparticle diffusion model.	354
Fig 8: Effect of temperature on DY removal by chitosan-iso-vanillin (DY=40 ppm, pH=3, W=0.05 g, t=3 h).	355
Table 1. Results of fitting the DY50 removal data to the Langmuir, Freundlich, and Temkin isotherms.	356
Table 2. Effect of adsorption dosage of chitosan-iso-vanillin on DY removal at pH 3.	357
Table 3. Pseudo-first-order and pseudo-second-order kinetic parameters.	358
Table 4. Thermodynamic parameters for DY removal on chitosan-iso-vanillin at different temperatures.	359

Figures

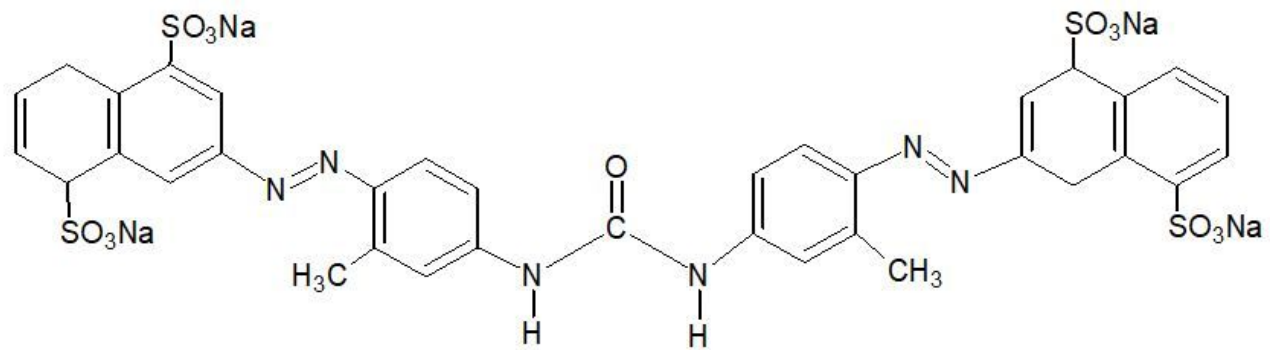


Figure 1

Structure of Direct Yellow 50 dye.

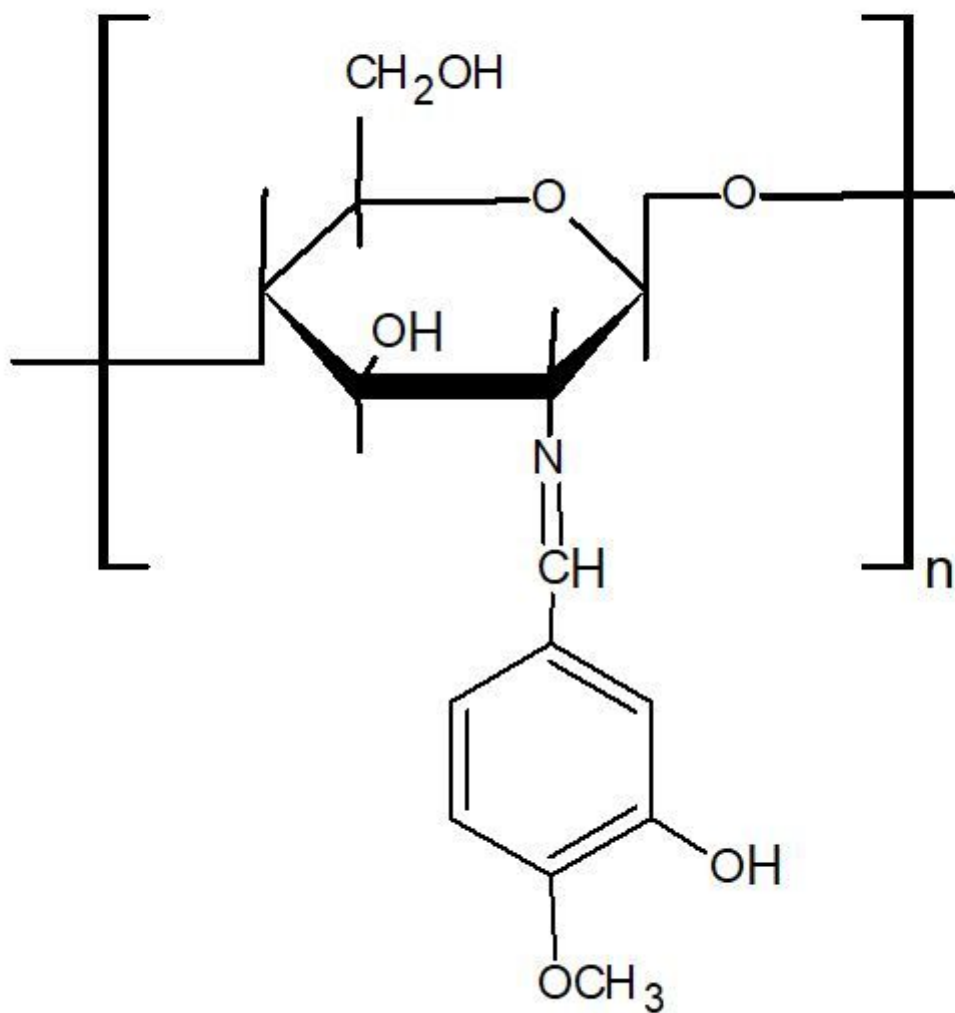


Figure 2

Structure of chitosan-iso-vanillin biosorbent.

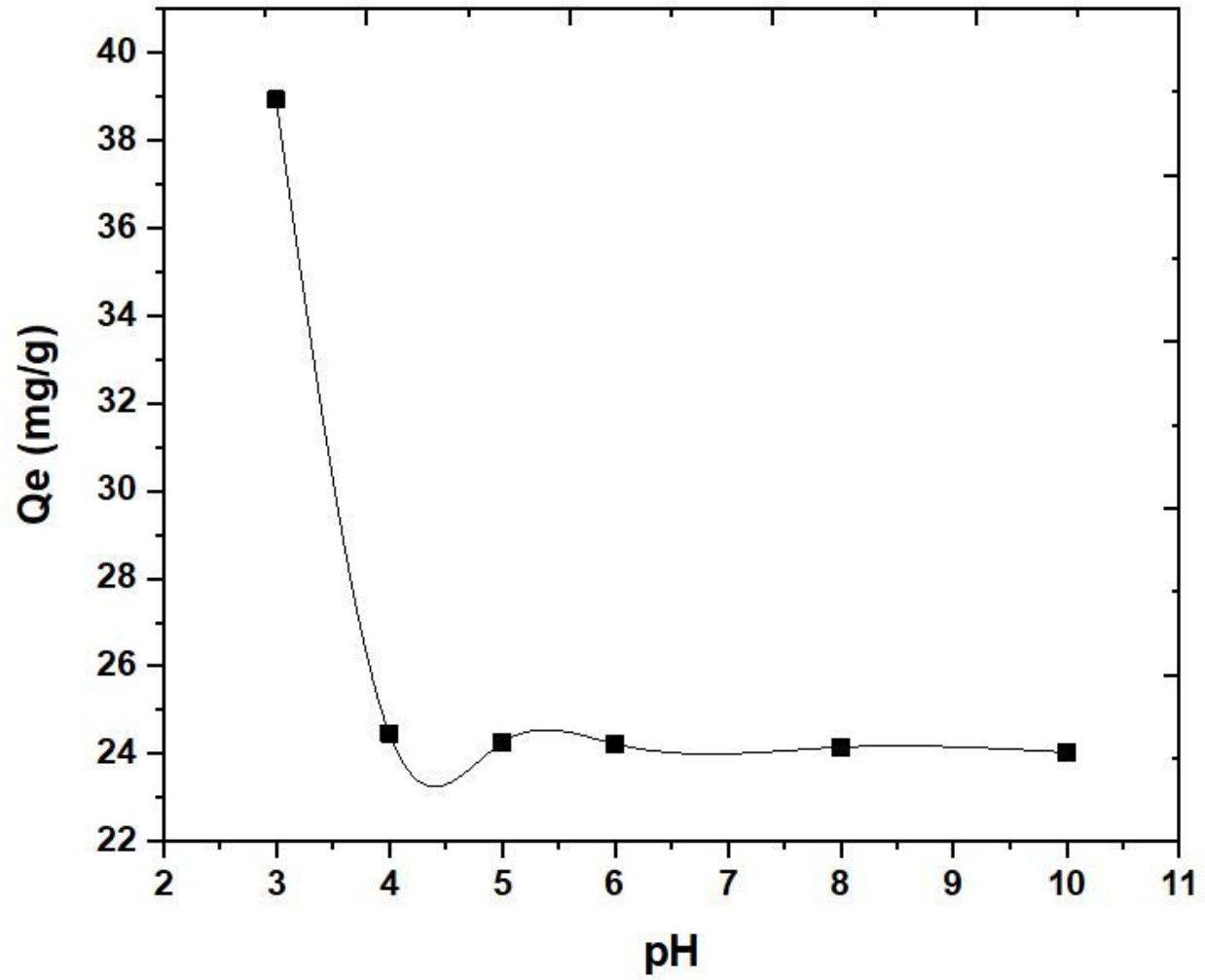


Figure 3

Effect of pH on DY removal by chitosan-iso-vanillin (DY=40 ppm, T=30°C, W=0.05 g and t=3 h).

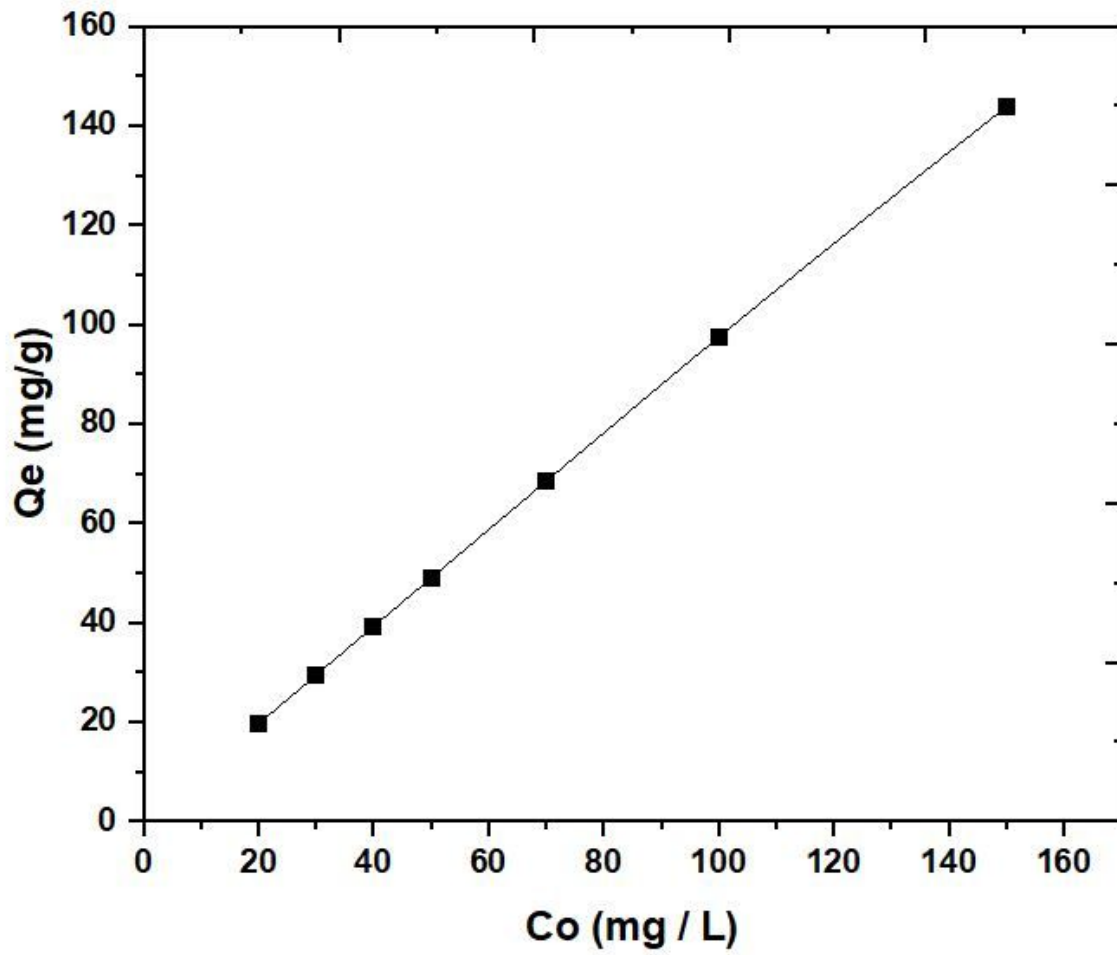


Figure 4

Effect of initial DY50 concentration on the equilibrium adsorption capacity of chitosan-iso-vanillin (W=0.05 g, pH=3, T=30°C, t=3 h).

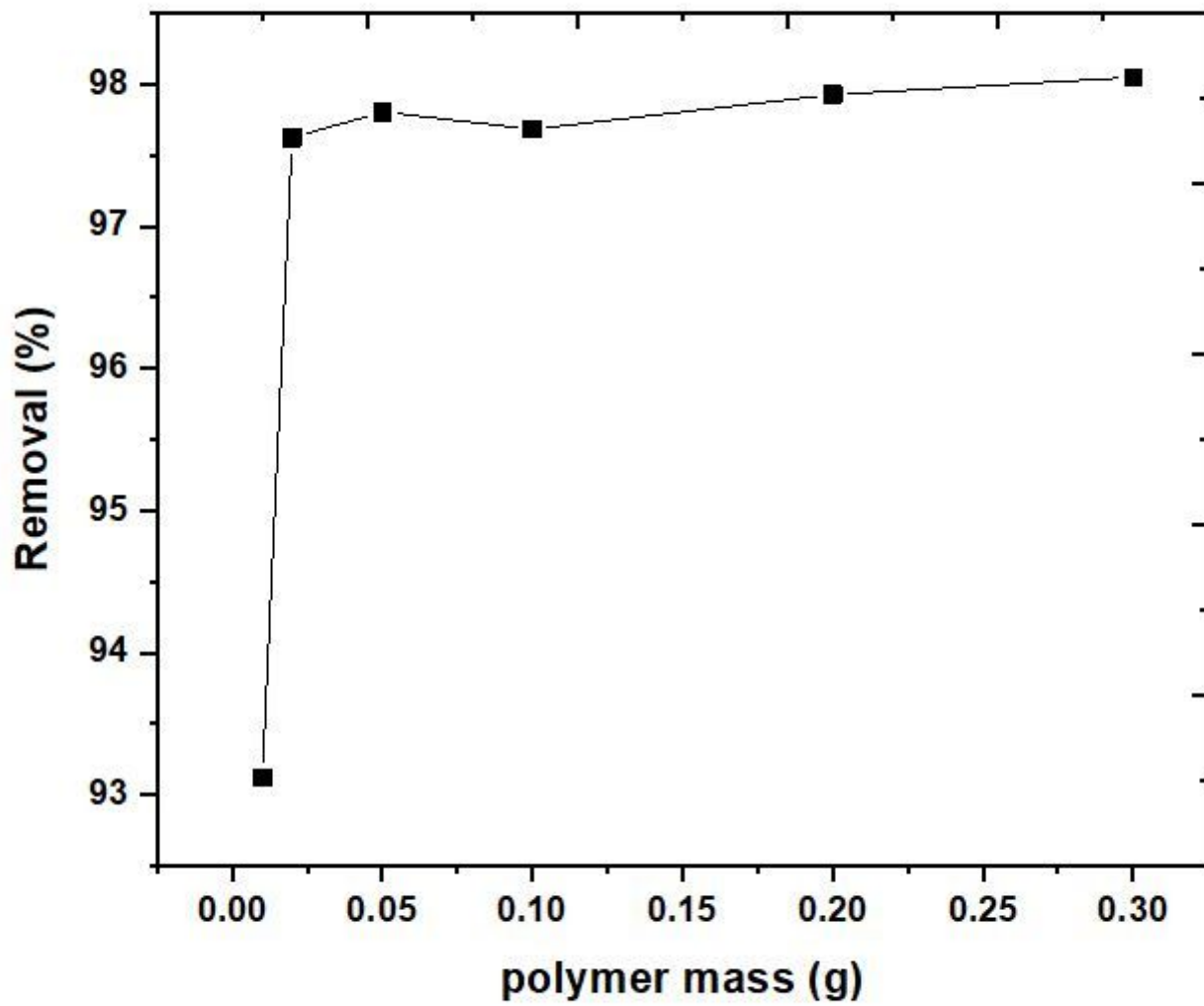


Figure 5

Effect of biosorbent dose on DY removal (DY=40 ppm, pH=3, T=30°C, t=3 h).

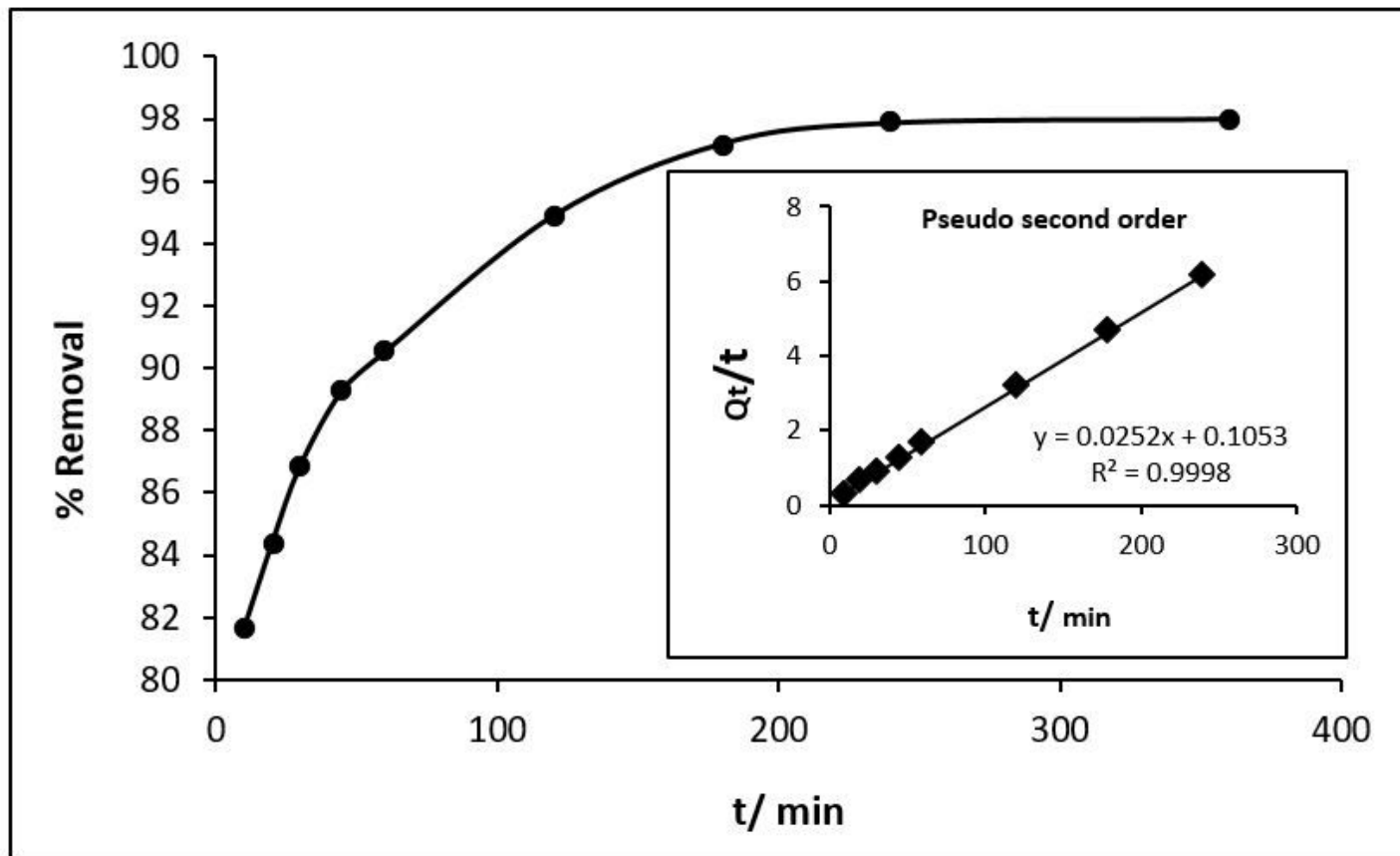


Figure 6

Effect of contact time on DY50 removal by chitosan-iso-vanillin (DY=40 ppm, pH=3, T=30°C, W=0.05 g).

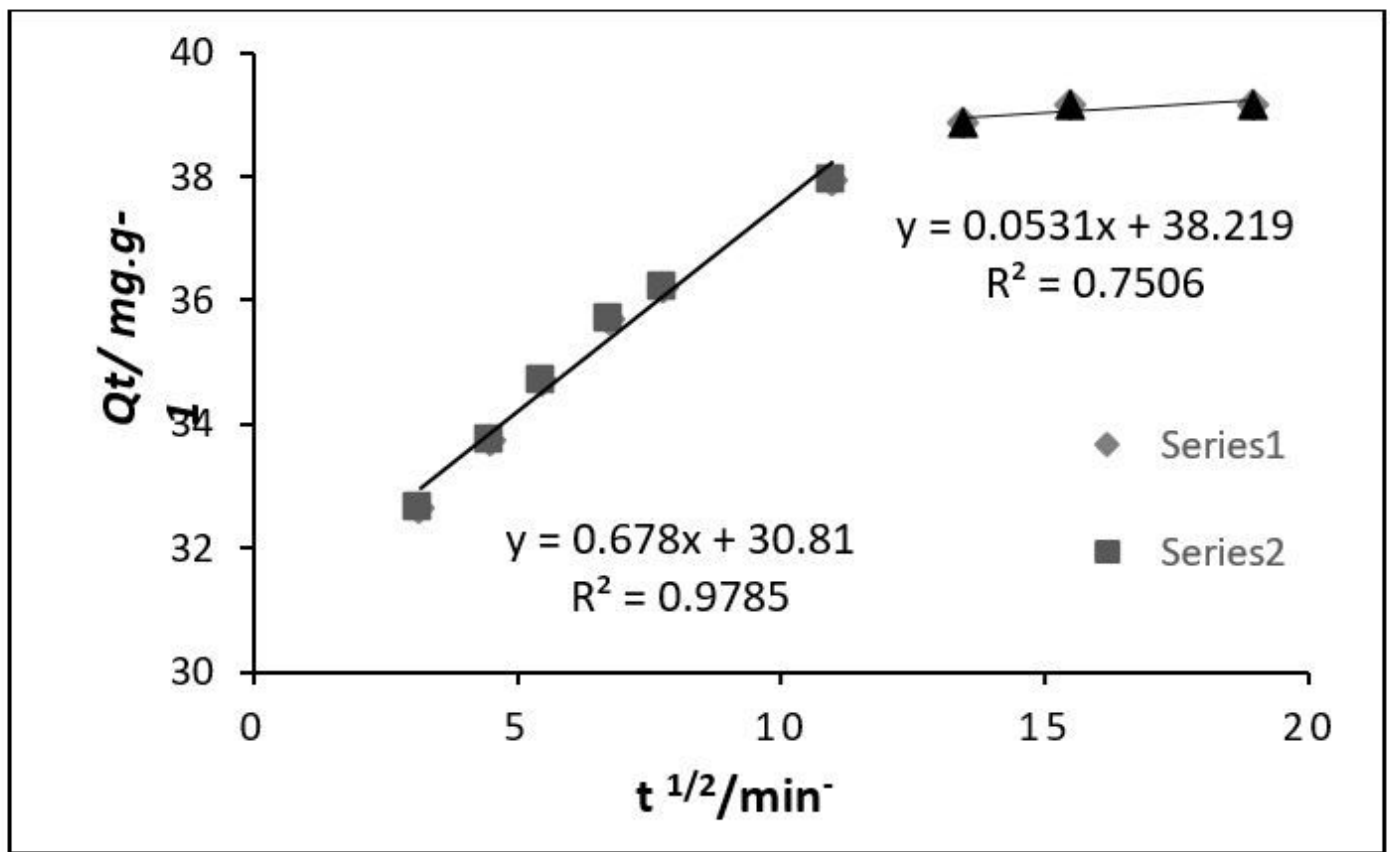


Figure 7

Fitting of DY adsorption data to the Weber-Morris intraparticle diffusion model.

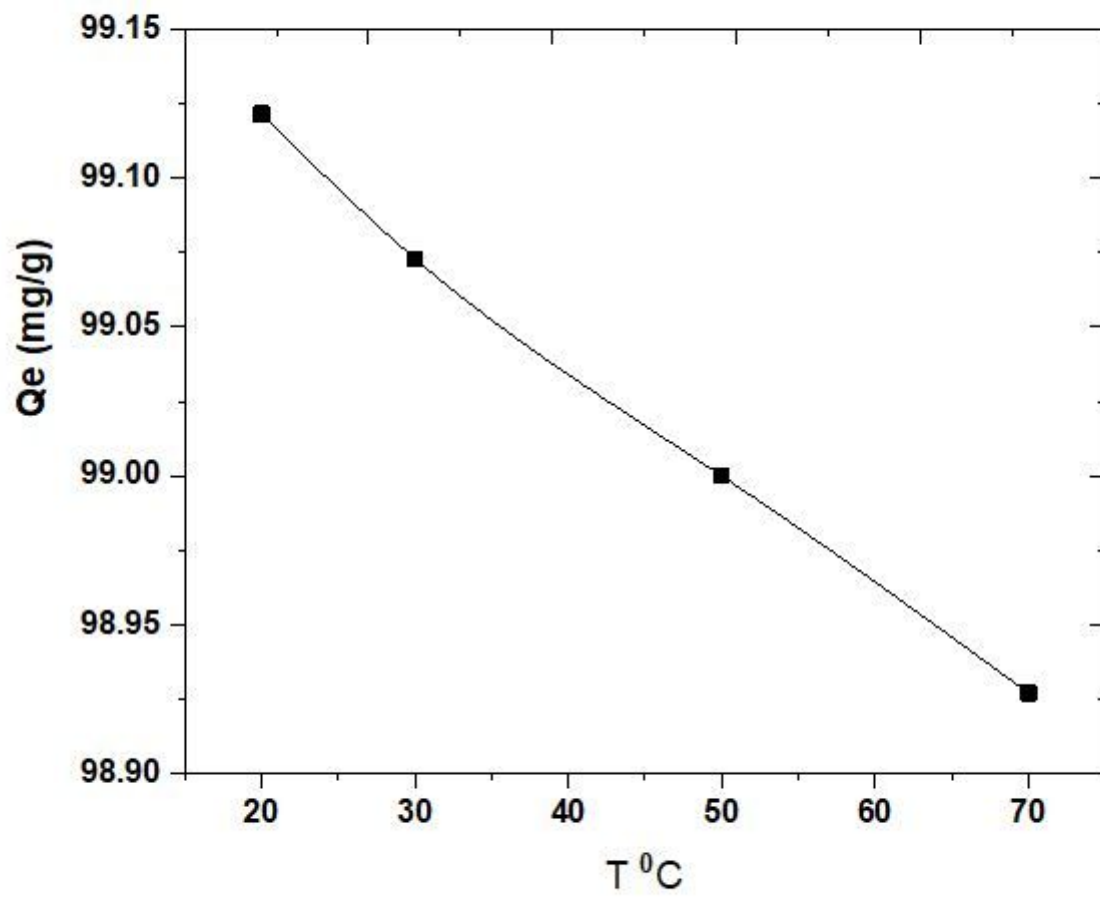


Figure 8

Effect of temperature on DY removal by chitosan-iso-vanillin (DY=40 ppm, pH=3, W=0.05 g, t=3 h).